

Hygrothermal analysis of antisymmetric cross-ply laminates using a refined plate theory

A. M. Zenkour · D. S. Mashat · R. A. Alghanmi

Received: 23 April 2013 / Accepted: 17 January 2014 / Published online: 29 January 2014
© Springer Science+Business Media Dordrecht 2014

Abstract The effect of hygrothermal conditions on the antisymmetric cross-ply laminates has been investigated using a unified shear deformation plate theory. The present plate theory enables the trial and testing of different through-the-thickness transverse shear-deformation distributions and, among them, strain distributions do not involve the undesirable implications of the transverse shear correction factors. The differential equations of laminated plates whose deformations are governed by either the shear deformation theories or the classical one are derived. Displacement functions that identically satisfy boundary conditions are used to reduce the governing equations to a set of coupled ordinary differential equations with variable coefficients. A wide variety of results is presented for the static response of simply supported rectangular plates under non-uniform sinusoidal hygrothermal/thermal loadings. The influence

of material anisotropy, aspect ratio, side-to-thickness ratio, thermal expansion coefficients ratio and stacking sequence on the hygrothermally induced response is studied.

Keywords Hygrothermal/thermal conditions · Unified theory · Anti-symmetric · Laminated plates

1 Introduction

The composite materials are widely used in civil, aerospace, automobile and other engineering fields due to their advantage of high stiffness and strength to weight ratio. With the ever-increasing applications of laminated composites in environmental conditions hygrothermal behavior of such laminates has attracted considerable attention. During the operational life, the variation of temperature and moisture reduces the elastic moduli and degrades the strength of the laminated material. As a result, a careful evaluation of the effects of environmental exposure is required to find the nature and extent of their deleterious effects upon performance.

Sai Ram and Sinha (1991, 1992) have studied the hygrothermal effects on the bending and free vibration behavior of laminated composite plates using the first-order shear deformation theory and employing finite element method. The effects of moisture and temperature on the deflections and stress resultants are

A. M. Zenkour (✉) · D. S. Mashat
Department of Mathematics, Faculty of Science, King Abdulaziz University, P.O. Box 80203, Jeddah 21589, Saudi Arabia
e-mail: zenkour@gmail.com

A. M. Zenkour
Department of Mathematics, Faculty of Science, Kafrelsheikh University, Kafr El-Sheikh 33516, Egypt

R. A. Alghanmi
Department of Mathematics, Rabigh College of Sciences and Arts, King Abdulaziz University, Jeddah, Saudi Arabia

presented for simply supported and clamped anti-symmetric cross-ply and angle-ply laminates using reduced lamina properties at elevated moisture concentration and temperature. Lee et al. (1992) have studied the influence of hygrothermal effects on the cylindrical bending of symmetric angle-ply laminated plates subjected to uniform transverse load for different boundary conditions via classical laminated plate theory and von-Karman's large deflection theory. The material properties of the composite are assumed to be independent of temperature and moisture variation. It has been observed that the classical laminated plate theory may not be adequate for the analysis of composite laminates even in the small deflection range. However, studies of temperature and moisture effects on the bending of rectangular plates based on the shear deformation theories are limited in number, and all these studies assumed perfectly initial configurations (Sai Ram and Sinha 1991, 1992; Pipes et al. 1976). Many studies based on classical plate theory of thin rectangular plates subjected to mechanical or thermal loading or their combinations as well as the hygrothermal effects are presented in the literature (Sai Ram and Sinha 1992; Whitney and Ashton 1971; Bahrami and Nosier 2007).

Rao and Sinha (2004) have studied the effects of moisture and temperature on the bending characteristics of thick multidirectional fibrous composite plates. The finite element analysis accounts for the hygrothermal strains and reduced elastic properties of multidirectional composites at an elevated moisture concentration and temperature. Deflections and stresses are evaluated for thick multidirectional composite plates under uniform and linearly varying through-the-thickness moisture concentration and temperature. Results reveal the effects of fiber directionality on deflection and stresses. Wang et al. (2005) have studied the response of dynamic interlaminar stresses in laminated composite plates with piezoelectric layers using an analytical approach. Benkhedda et al. (2008) have proposed an analytical approach to calculate the hygrothermal stresses in laminated composite plates, and took into account the change of mechanical characteristics due to moisture and temperature. In their study, the distribution of the transient in-plane stresses through the thickness of laminates is presented, whereas the transverse stresses were not taken into account. Ameer et al. (2009) have analyzed the problem of interfacial stresses in steel

beams strengthened with bonded hygrothermal aged composite laminates by using linear elastic theory. From the literatures reviewed, it can be found that the research on local hygrothermal stresses of cross-ply laminates and sandwich plates subjected to temperature and moisture effects seems to be lacking, which is the problem to be addressed in this paper.

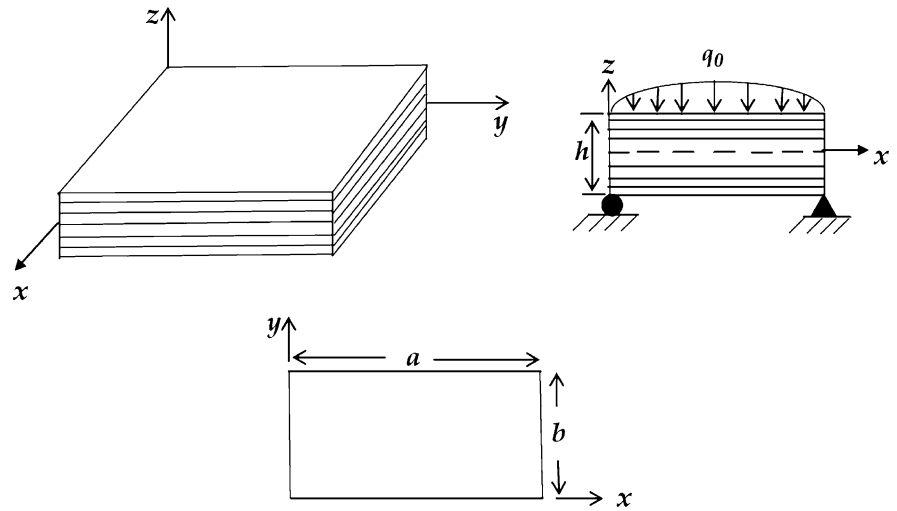
The so-called equivalent single-layer models, such as classical and shear deformation theories, have been developed for the analysis of laminated plates. There are additional models have effectively been employed in developing a two-dimensional model for laminated plates, which is capable of determining the in-plane and interlaminar stresses such as the layerwise (Reddy 1987) and zig-zag (Carrera 2003 and all references therein) theories. The object of this paper is to study the deflections and stresses of antisymmetric cross-ply laminates under sinusoidally non-uniform distribution temperature and/or sinusoidally non-uniform distribution moisture and/or sinusoidally distributed transverse mechanical load. A unified theory that takes into account the effect of transverse normal strain of laminated composite plates is presented. The governing equations are converted into a single-order system of the equations. Analytical solutions for simply supported laminated plates are developed using the Navier's procedure and separation of variable technique. Numerical results for deflection and stresses are presented.

2 Theoretical development

Consider a fiber reinforced rectangular laminated plate occupying the region $[0, a] \times [0, b] \times [-h/2, +h/2]$ in the unstressed reference configuration (see Fig. 1). The mid-plane is defined by $z = 0$ and its external bounding planes being defined by $z = \pm h/2$. The plate composed of n orthotropic layers oriented at angles $\theta_1, \theta_2, \dots, \theta_n$. The material of each layer is assumed to possess one plane of elastic symmetry parallel to the x - y plane. Perfect bonding between the orthotropic layers and temperature-independent mechanical, thermal and moisture properties are assumed. The plate subjected to a transverse static mechanical load $q(x, y)$ and temperature field $T(x, y, z)$ as well as moisture concentration $C(x, y, z)$.

The displacement field at a point (x, y, z) in the laminated plate can be expressed as (Zenkour 2005b, 2007, 2008):

Fig. 1 Coordinate system and schematic diagram for the plate



$$\left. \begin{aligned} u_x(x, y, z) &= u - z \frac{\partial w}{\partial x} + \Psi(z)\phi_x, \\ u_y(x, y, z) &= v - z \frac{\partial w}{\partial y} + \Psi(z)\phi_y, \\ u_z(x, y, z) &= w + \Psi'(z)\phi_z, \end{aligned} \right\} \quad (1)$$

where (u_x, u_y, u_z) are the displacements along $x, y,$ and z directions, respectively; (u, v, w) are the in-plane displacements; (ϕ_x, ϕ_y) are rotations of the normal to the middle plane about y -axes and x -axes, respectively; ϕ_z is additional displacement account for the effect of normal stress. All of the generalized displacements $(u, v, w, \phi_x, \phi_y, \phi_z)$ are functions of x and y . The displacement field can be obtained in the case of classical plate theory (CPT) by putting:

$$\Psi(z) = 0 \quad \text{and} \quad \phi_z = 0, \quad (2)$$

the case of first-order (or uniform) shear deformation plate theory (FPT) by putting:

$$\Psi(z) = z \quad \text{and} \quad \phi_z = 0. \quad (3)$$

However, the displacement field can be obtained in the case of higher-order shear deformation plate theory (HPT) (see Reddy 1984) by putting:

$$\Psi(z) = z \left[1 - \frac{1}{3} \left(\frac{z}{h/2} \right)^2 \right] \quad \text{and} \quad \phi_z = 0. \quad (4)$$

Many refined theories are given by taking different forms of $\Psi(z)$ (see, e.g., Atmane et al. 2010). In the case of simple sinusoidal shear deformation plate theory (SPT) (Zenkour 2004a, b, c, 2005a, 2006; Zenkour et al. 2013) by putting:

$$\Psi(z) = \frac{h}{\pi} \sin\left(\frac{\pi z}{h}\right) \quad \text{and} \quad \phi_z = 0. \quad (5)$$

Finally, the displacement field can be obtained in the case of refined sinusoidal shear deformation plate theory (RPT) (Zenkour 2007) by putting:

$$\Psi(z) = \frac{h}{\pi} \sin\left(\frac{\pi z}{h}\right) \quad \text{and} \quad \phi_z \neq 0. \quad (6)$$

Note that, no shear correction factors are needed in computing the shear stresses for HPT, SPT and RPT, because a correct representation of the transverse shearing strain is given.

The strains compatible with the displacements field given in Eq. (1) can be expressed as

$$\left\{ \begin{matrix} \varepsilon_{xx} \\ \varepsilon_{yy} \\ \gamma_{xy} \end{matrix} \right\} = \left\{ \begin{matrix} \varepsilon_{xx}^0 \\ \varepsilon_{yy}^0 \\ \gamma_{xy}^0 \end{matrix} \right\} + z \left\{ \begin{matrix} \kappa_{xx} \\ \kappa_{yy} \\ \kappa_{xy} \end{matrix} \right\} + \Psi(z) \left\{ \begin{matrix} \eta_{xx} \\ \eta_{yy} \\ \eta_{xy} \end{matrix} \right\},$$

$$\varepsilon_{zz} = \Psi''(z)\varepsilon_{zz}^0, \quad \left\{ \begin{matrix} \gamma_{yz} \\ \gamma_{xz} \end{matrix} \right\} = \Psi'(z) \left\{ \begin{matrix} \gamma_{yz}^0 \\ \gamma_{xz}^0 \end{matrix} \right\},$$

where

$$\begin{aligned} \varepsilon_{xx}^0 &= \frac{\partial u}{\partial x}, & \varepsilon_{yy}^0 &= \frac{\partial v}{\partial y}, & \gamma_{xy}^0 &= \frac{\partial v}{\partial x} + \frac{\partial u}{\partial y}, \\ \gamma_{yz}^0 &= \phi_y + \frac{\partial \phi_z}{\partial y}, & \gamma_{xz}^0 &= \phi_x + \frac{\partial \phi_z}{\partial x}, & \varepsilon_{zz}^0 &= \phi_z, \\ \kappa_{xx} &= -\frac{\partial^2 w}{\partial x^2}, & \kappa_{yy} &= -\frac{\partial^2 w}{\partial y^2}, & \kappa_{xy} &= -2\frac{\partial^2 w}{\partial x \partial y}, \\ \eta_{xx} &= \frac{\partial \phi_x}{\partial x}, & \eta_{yy} &= \frac{\partial \phi_y}{\partial y}, & \eta_{xy} &= \frac{\partial \phi_y}{\partial x} + \frac{\partial \phi_x}{\partial y}. \end{aligned} \quad (8)$$

Each lamina in the laminated plate is assumed to be in a three-dimensional stress state so that the constitutive relations for a typical lamina k can be written as

$$\begin{Bmatrix} \sigma_{xx} \\ \sigma_{yy} \\ \sigma_{zz} \\ \tau_{yz} \\ \tau_{xz} \\ \tau_{xy} \end{Bmatrix}^k = \begin{bmatrix} c_{11} & c_{12} & c_{13} & 0 & 0 & c_{16} \\ c_{12} & c_{22} & c_{23} & 0 & 0 & c_{26} \\ c_{13} & c_{23} & c_{33} & 0 & 0 & c_{36} \\ 0 & 0 & 0 & c_{44} & c_{45} & 0 \\ 0 & 0 & 0 & c_{45} & c_{55} & 0 \\ c_{16} & c_{26} & c_{36} & 0 & 0 & c_{66} \end{bmatrix}^k \times \begin{Bmatrix} \varepsilon_{xx} - \alpha_x \Delta T - \beta_x \Delta C \\ \varepsilon_{yy} - \alpha_y \Delta T - \beta_y \Delta C \\ \varepsilon_{zz} - \alpha_z \Delta T - \beta_z \Delta C \\ \gamma_{yz} \\ \gamma_{xz} \\ \gamma_{xy} - \alpha_{xy} \Delta T - \beta_{xy} \Delta C \end{Bmatrix}^k, \tag{9}$$

where $c_{ij}^{(k)}$ are the transformed elastic coefficients; $\Delta T = T - T_0$, $\Delta C = C - C_0$ in which $T \equiv T(x, y, z)$ is the temperature distribution, T_0 is the reference temperature and $C \equiv C(x, y, z)$ is the moisture distribution, C_0 is the reference moisture concentration; $\alpha_x, \alpha_y, \alpha_z$ and α_{xy} are the thermal expansion coefficients and $\beta_x, \beta_y, \beta_z$ and β_{xy} are the moisture concentration coefficients.

3 Governing equations of equilibrium

The equilibrium equations can be derived by using the principle of virtual that yields

$$\int_{-h/2}^{h/2} \int_{\Omega} \left[\sigma_{xx}^{(k)} \delta \varepsilon_{xx} + \sigma_{yy}^{(k)} \delta \varepsilon_{yy} + \sigma_{zz}^{(k)} \delta \varepsilon_{zz} + \tau_{xy}^{(k)} \delta \gamma_{xy} + \tau_{yz}^{(k)} \delta \gamma_{yz} + \tau_{xz}^{(k)} \delta \gamma_{xz} \right] d\Omega dz - \int_{\Omega} q(x, y) \delta w d\Omega = 0. \tag{10}$$

Integrating the displacement gradients in Eq. (10) by parts and setting the coefficients of $\delta u, \delta v, \delta w, \delta \phi_x, \delta \phi_y$ and $\delta \phi_z$ to zero separately, we obtain the equilibrium equations as

$$\begin{aligned} \frac{\partial N_{xx}}{\partial x} + \frac{\partial N_{xy}}{\partial y} = 0, \quad \frac{\partial N_{xy}}{\partial x} + \frac{\partial N_{yy}}{\partial y} = 0, \\ \frac{\partial^2 M_{xx}}{\partial x^2} + 2 \frac{\partial^2 M_{xy}}{\partial x \partial y} + \frac{\partial^2 M_{yy}}{\partial y^2} + q = 0, \\ \frac{\partial S_{xx}}{\partial x} + \frac{\partial S_{xy}}{\partial y} - Q_{xz} = 0, \quad \frac{\partial S_{xy}}{\partial x} + \frac{\partial S_{yy}}{\partial y} - Q_{yz} = 0, \\ \frac{\partial Q_{xz}}{\partial x} + \frac{\partial Q_{yz}}{\partial y} - N_{zz} = 0, \end{aligned} \tag{11}$$

where

$$\begin{Bmatrix} N_{xx}, N_{yy}, N_{xy} \\ M_{xx}, M_{yy}, M_{xy} \\ S_{xx}, S_{yy}, S_{xy} \end{Bmatrix} = \sum_{k=1}^n \int_{z_k}^{z_{k+1}} \begin{Bmatrix} \sigma_{xx}^{(k)} \\ \sigma_{yy}^{(k)} \\ \tau_{xy}^{(k)} \end{Bmatrix} dz, \tag{12}$$

$$\begin{Bmatrix} 1 \\ z \\ \Psi(z) \end{Bmatrix} dz, \quad N_{zz} = \sum_{k=1}^n \int_{z_k}^{z_{k+1}} \sigma_{zz}^{(k)} \Psi''(z) dz,$$

$$(Q_{xz}, Q_{yz}) = \sum_{k=1}^n \int_{z_k}^{z_{k+1}} \begin{Bmatrix} \tau_{xz}^{(k)} \\ \tau_{yz}^{(k)} \end{Bmatrix} \Psi'(z) dz.$$

Using Eq. (9) in Eq. (12), we can write the stress resultants functions N , the stress couples M , the additional stress couples S , the transverse shear stress resultants Q and the transverse normal stress resultant N_{zz} as:

$$\begin{Bmatrix} N \\ M \\ S \end{Bmatrix} = \begin{bmatrix} A & B & B^a \\ B & D & D^a \\ B^a & D^a & F^a \end{bmatrix} \begin{Bmatrix} \varepsilon \\ \kappa \\ \eta \end{Bmatrix} - \begin{Bmatrix} N^H \\ M^H \\ S^H \end{Bmatrix},$$

$$Q = A^a \gamma, \quad N_{zz} = [L^a \quad \bar{L} \quad \hat{L}] \begin{Bmatrix} \varepsilon \\ \kappa \\ \eta \end{Bmatrix} + \tilde{L}_{33} \varepsilon_{zz}^0 - N_{zz}^H, \tag{13}$$

where

$$\begin{aligned} N &= \{N_{xx}, N_{yy}, N_{xy}\}^t, \quad M = \{M_{xx}, M_{yy}, M_{xy}\}^t, \\ S &= \{S_{xx}, S_{yy}, S_{xy}\}^t, \quad N^H = \{N_{xx}^H, N_{yy}^H, N_{xy}^H\}^t, \\ M^H &= \{M_{xx}^H, M_{yy}^H, M_{xy}^H\}^t, \quad S^H = \{S_{xx}^H, S_{yy}^H, S_{xy}^H\}^t, \\ \varepsilon &= \{\varepsilon_{xx}^0, \varepsilon_{yy}^0, \gamma_{xy}^0\}^t, \quad \kappa = \{\kappa_{xx}, \kappa_{yy}, \kappa_{xy}\}^t, \\ \eta &= \{\eta_{xx}, \eta_{yy}, \eta_{xy}\}^t, \end{aligned} \tag{14}$$

and

$$\begin{aligned} A &= \begin{bmatrix} A_{11} & A_{12} & A_{16} \\ A_{12} & A_{22} & A_{26} \\ A_{16} & A_{26} & A_{66} \end{bmatrix}, \quad B = \begin{bmatrix} B_{11} & B_{12} & B_{16} \\ B_{12} & B_{22} & B_{26} \\ B_{16} & B_{26} & B_{66} \end{bmatrix}, \\ D &= \begin{bmatrix} D_{11} & D_{12} & D_{16} \\ D_{12} & D_{22} & D_{26} \\ D_{16} & D_{26} & D_{66} \end{bmatrix}, \quad B^a = \begin{bmatrix} B_{11}^a & B_{12}^a & B_{16}^a \\ B_{12}^a & B_{22}^a & B_{26}^a \\ B_{16}^a & B_{26}^a & B_{66}^a \end{bmatrix}, \\ D^a &= \begin{bmatrix} D_{11}^a & D_{12}^a & D_{16}^a \\ D_{12}^a & D_{22}^a & D_{26}^a \\ D_{16}^a & D_{26}^a & D_{66}^a \end{bmatrix}, \quad F^a = \begin{bmatrix} F_{11}^a & F_{12}^a & F_{16}^a \\ F_{12}^a & F_{22}^a & F_{26}^a \\ F_{16}^a & F_{26}^a & F_{66}^a \end{bmatrix}. \end{aligned} \tag{15}$$

Note that “t” denotes the transpose of the given vector. The laminate stiffness coefficients A_{ij} and B_{ij} , ... etc., are given in terms of $c_{ij}^{(k)}$ for the layers $k = 1, 2, \dots, n$ as:

$$\begin{aligned} \{A_{ij}, B_{ij}, D_{ij}\} &= \sum_{k=1}^n \int_{z_k}^{z_{k+1}} c_{ij}^{(k)} \{1, z, z^2\} dz, \quad (i, j = 1, 2, 6), \\ A_{ij}^a &= \sum_{k=1}^n \int_{z_k}^{z_{k+1}} c_{ij}^{(k)} [\Psi'(z)]^2 dz, \quad (i, j = 4, 5), \\ \{B_{ij}^a, D_{ij}^a, F_{ij}^a\} &= \sum_{k=1}^n \int_{z_k}^{z_{k+1}} c_{ij}^{(k)} \{1, z, \Psi(z)\} \Psi(z) dz, \\ &\quad (i, j = 1, 2, 6), \\ \{L_{i3}^a, \bar{L}_{i3}, \hat{L}_{i3}\} &= \sum_{k=1}^n \int_{z_k}^{z_{k+1}} c_{i3}^{(k)} \{1, z, \Psi(z)\} \Psi''(z) dz, \\ &\quad (i = 1, 2, 6), \\ \tilde{L}_{33} &= \sum_{k=1}^n \int_{z_k}^{z_{k+1}} c_{33}^{(k)} [\Psi'(z)]^2 dz. \end{aligned} \tag{16}$$

The stress and moment resultants $N_{xx}^H, M_{xx}^H \dots$ etc., due to the hygrothermal loading are defined by:

$$\begin{aligned} \begin{Bmatrix} N_{xx}^H, M_{xx}^H, S_{xx}^H \\ N_{yy}^H, M_{yy}^H, S_{yy}^H \\ N_{xy}^H, M_{xy}^H, S_{xy}^H \end{Bmatrix} &= \sum_{k=1}^n \int_{z_k}^{z_{k+1}} \begin{bmatrix} c_{11} & c_{12} & c_{13} & c_{16} \\ c_{12} & c_{22} & c_{23} & c_{26} \\ c_{13} & c_{23} & c_{33} & c_{36} \\ c_{16} & c_{26} & c_{36} & c_{66} \end{bmatrix}^{(k)} \begin{Bmatrix} \alpha_x \Delta T + \beta_x \Delta C \\ \alpha_y \Delta T + \beta_y \Delta C \\ \alpha_z \Delta T + \beta_z \Delta C \\ \alpha_{xy} \Delta T + \beta_{xy} \Delta C \end{Bmatrix} \times (1, z, \Psi(z)) dz, \\ N_{zz}^H &= \sum_{k=1}^n \int_{z_k}^{z_{k+1}} [c_{13} \quad c_{23} \quad c_{33} \quad c_{36}]^{(k)} \begin{Bmatrix} \alpha_x \Delta T + \beta_x \Delta C \\ \alpha_y \Delta T + \beta_y \Delta C \\ \alpha_z \Delta T + \beta_z \Delta C \\ \alpha_{xy} \Delta T + \beta_{xy} \Delta C \end{Bmatrix} \Psi''(z) dz. \end{aligned} \tag{17}$$

Consistent with the present unified plate theory, the temperature variation and the moisture concentration through the thickness are, respectively, assumed to be

$$\begin{aligned} T(x, y, z) &= T_1(x, y) + \frac{z}{h} T_2(x, y) + \frac{\Psi(z)}{h} T_3(x, y), \\ C(x, y, z) &= C_1(x, y) + \frac{z}{h} C_2(x, y) + \frac{\Psi(z)}{h} C_3(x, y), \end{aligned} \tag{18}$$

where T_m and $C_m (m = 1, 2, 3)$ are the thermal loads and moisture concentration factors, respectively.

Substituting Eq. (13) into Eq. (11), one obtains the following operator equation,

$$[L]\{\delta\} = \{f\}, \tag{19}$$

where $\{\delta\}$ and $\{f\}$ denote the columns

$$\begin{aligned} \{\delta\} &= \{u, v, w, \varphi_x, \varphi_y, \varphi_z\}^t, \{f\} \\ &= \{f_1, f_2, f_3, f_4, f_5, f_6\}^t. \end{aligned} \tag{20}$$

The elements of the symmetric matrix $[L]$ are given in Appendix 1. The components of the generalized force vector $\{f\}$ are given by:

$$\begin{aligned} f_1 &= \frac{\partial N_{xx}^H}{\partial x} + \frac{\partial N_{xy}^H}{\partial y}, \quad f_2 = \frac{\partial N_{xy}^H}{\partial x} + \frac{\partial N_{yy}^H}{\partial y}, \\ f_3 &= q - \frac{\partial^2 M_{xx}^H}{\partial x^2} - 2 \frac{\partial^2 M_{xy}^H}{\partial x \partial y} - \frac{\partial^2 M_{yy}^H}{\partial y^2}, \\ f_4 &= \frac{\partial S_x^H}{\partial x} + \frac{\partial S_{xy}^H}{\partial y}, \quad f_5 = \frac{\partial S_{xy}^H}{\partial x} + \frac{\partial S_y^H}{\partial y}, \quad f_6 = N_{zz}^H. \end{aligned} \tag{21}$$

4 Analytical solution

For simply supported laminates the following boundary conditions are imposed at the side edges,

$$\begin{aligned} v = w = \varphi_y = \varphi_z = N_x = M_x = S_x = 0 &\quad \text{at } x = 0, a, \\ u = w = \varphi_x = \varphi_z = N_y = M_y = S_y = 0 &\quad \text{at } y = 0, b. \end{aligned} \tag{22}$$

We assume that the applied transverse load q , the transverse temperature loads T_m and the moisture concentration C_m can be expressed as:

$$\begin{Bmatrix} q \\ T_m \\ C_m \end{Bmatrix} = \begin{Bmatrix} q_0 \\ \bar{T}_m \\ \bar{C}_m \end{Bmatrix} \sin(\lambda x) \sin(\mu y), \quad m = 1, 2, 3, \tag{23}$$

where $\lambda = i\pi/a$, $\mu = j\pi/b$ in which i and j are mode numbers and q_0 represents the initial mechanical load. There are three specific co-ordinates transformations under which an orthotropic material retains monoclinic symmetry, namely, rotations about the axes x , y or z . The transformation formulae for the stiffness $c_{ij}^{(k)}$ are given in Appendix 2.

If the plate construction is cross-ply, i.e., θ_k should be either 0° or 90° , then the following plate stiffness coefficients are identically zero:

$$\begin{aligned} A_{16} = A_{26} = A_{45}^a = 0, \quad B_{16} = B_{26} = 0, \\ B_{16}^a = B_{26}^a = 0, \quad D_{16} = D_{26} = 0, \\ D_{16}^a = D_{26}^a = 0, \quad F_{16}^a = F_{26}^a = 0, \\ L_{63}^a = \bar{L}_{63} = \hat{L}_{63} = 0. \end{aligned} \tag{24}$$

In addition, the thermal expansion coefficient α_{xy} and the moisture concentration coefficient β_{xy} vanishes, i.e., $\alpha_{xy} = 0$ and $\beta_{xy} = 0$.

Following the Navier’s solution procedure, we assume the following form for displacements that satisfy the boundary conditions,

$$\begin{Bmatrix} u \\ v \\ w \\ \varphi_x \\ \varphi_y \\ \varphi_z \end{Bmatrix} = \sum_{i=1}^{\infty} \sum_{j=1}^{\infty} \begin{Bmatrix} U_{ij} \cos(\lambda x) \sin(\mu y) \\ V_{ij} \sin(\lambda x) \cos(\mu y) \\ W_{ij} \sin(\lambda x) \sin(\mu y) \\ X_{ij} \cos(\lambda x) \sin(\mu y) \\ Y_{ij} \sin(\lambda x) \cos(\mu y) \\ Z_{ij} \sin(\lambda x) \sin(\mu y) \end{Bmatrix}, \tag{25}$$

where U_{ij} , V_{ij} , W_{ij} , X_{ij} , Y_{ij} and Z_{ij} are arbitrary parameters. Substituting Eq. (25) into Eq. (19), one obtains the following operator equation,

$$[C]\{\Delta\} = \{F\}, \tag{26}$$

where $\{\Delta\}$ and $\{F\}$ denote the columns

$$\begin{aligned} \{\Delta\} &= \{U_{ij}, V_{ij}, W_{ij}, X_{ij}, Y_{ij}, Z_{ij}\}^t, \\ \{F\} &= \{F_1^{ij}, F_2^{ij}, F_3^{ij}, F_4^{ij}, F_5^{ij}, F_6^{ij}\}^t. \end{aligned} \tag{27}$$

The components of the generalized force vector $\{F\}$ and the elements of the symmetric matrix $[C]$ are given in Appendix 3.

The stress components for the RPT are

$$\begin{aligned} \sigma_{xx}^{(k)} = & - \left\{ c_{11}^{(k)} \lambda U_{ij} + c_{12}^{(k)} \mu V_{ij} - z \left(c_{11}^{(k)} \lambda^2 + c_{12}^{(k)} \mu^2 \right) W_{ij} \right. \\ & + \Psi(z) \cdot \left(c_{11}^{(k)} \lambda X_{ij} + c_{12}^{(k)} \mu Y_{ij} \right) + c_{13}^{(k)} \Psi''(z) Z_{ij} \\ & + \left(c_{11}^{(k)} \alpha_x + c_{12}^{(k)} \alpha_y \right) [\bar{T}_1 + \bar{z} \bar{T}_2 + \bar{\Psi}(z) \bar{T}_3 - T_0] \\ & \left. + \left(c_{11}^{(k)} \beta_x + c_{12}^{(k)} \beta_y \right) [\bar{C}_1 + \bar{z} \bar{C}_2 + \bar{\Psi}(z) \bar{C}_3 - C_0] \right\} \\ & \times \sin(\lambda x) \sin(\mu y), \end{aligned} \tag{28a}$$

$$\begin{aligned} \sigma_{yy}^{(k)} = & - \left\{ c_{12}^{(k)} \lambda U_{ij} + c_{22}^{(k)} \mu V_{ij} - z \left(c_{12}^{(k)} \lambda^2 + c_{22}^{(k)} \mu^2 \right) W_{ij} \right. \\ & + \Psi(z) \cdot \left(c_{12}^{(k)} \lambda X_{ij} + c_{22}^{(k)} \mu Y_{ij} \right) + c_{23}^{(k)} \Psi''(z) Z_{ij} \\ & + \left(c_{12}^{(k)} \alpha_x + c_{22}^{(k)} \alpha_y \right) [\bar{T}_1 + \bar{z} \bar{T}_2 + \bar{\Psi}(z) \bar{T}_3 - T_0] \\ & \left. + \left(c_{12}^{(k)} \beta_x + c_{22}^{(k)} \beta_y \right) [\bar{C}_1 + \bar{z} \bar{C}_2 + \bar{\Psi}(z) \bar{C}_3 - C_0] \right\} \\ & \times \sin(\lambda x) \sin(\mu y), \end{aligned} \tag{28b}$$

$$\begin{aligned} \sigma_{zz}^{(k)} = & - \left\{ c_{13}^{(k)} \lambda U_{ij} + c_{23}^{(k)} \mu V_{ij} - z \left(c_{13}^{(k)} \lambda^2 + c_{23}^{(k)} \mu^2 \right) W_{ij} \right. \\ & + \Psi(z) \cdot \left(c_{13}^{(k)} \lambda X_{ij} + c_{23}^{(k)} \mu Y_{ij} \right) + c_{33}^{(k)} \Psi''(z) Z_{ij} \\ & + \left(c_{13}^{(k)} \alpha_x + c_{23}^{(k)} \alpha_y \right) [\bar{T}_1 + \bar{z} \bar{T}_2 + \bar{\Psi}(z) \bar{T}_3 - T_0] \\ & \left. + \left(c_{13}^{(k)} \beta_x + c_{23}^{(k)} \beta_y \right) [\bar{C}_1 + \bar{z} \bar{C}_2 + \bar{\Psi}(z) \bar{C}_3 - C_0] \right\} \\ & \times \sin(\lambda x) \sin(\mu y), \end{aligned} \tag{28c}$$

$$\begin{aligned} \tau_{xy}^{(k)} = & c_{66}^{(k)} \{ \mu U_{ij} + \lambda V_{ij} - 2z \lambda \mu W_{ij} + \Psi(z) \\ & \times (\mu X_{ij} + \lambda Y_{ij}) \} \cos(\lambda x) \cos(\mu y), \end{aligned} \tag{28d}$$

$$\tau_{yz}^{(k)} = c_{44}^{(k)} \Psi'(z) Y_{ij} \sin(\lambda x) \cos(\mu y), \tag{28e}$$

$$\tau_{xz}^{(k)} = c_{55}^{(k)} \Psi'(z) X_{ij} \cos(\lambda x) \sin(\mu y). \tag{28f}$$

The above stresses may be suitable for the FPT, HPT and SPT when the transverse normal stress is ignored and setting $Z_{ij} = 0$. However, one gets for the CPT only

$$\begin{aligned} \sigma_{xx}^{(k)} = & - \left\{ c_{11}^{(k)} \lambda U_{ij} + c_{12}^{(k)} \mu V_{ij} - z \left(c_{11}^{(k)} \lambda^2 + c_{12}^{(k)} \mu^2 \right) W_{ij} \right. \\ & + \Psi(z) \cdot \left(c_{11}^{(k)} \lambda X_{ij} + c_{12}^{(k)} \mu Y_{ij} \right) + \left(c_{11}^{(k)} \alpha_x + c_{12}^{(k)} \alpha_y \right) \\ & \times [\bar{T}_1 + \bar{z} \bar{T}_2 - T_0] + \left(c_{11}^{(k)} \beta_x + c_{12}^{(k)} \beta_y \right) \\ & \left. \times [\bar{C}_1 + \bar{z} \bar{C}_2 - C_0] \right\} \sin(\lambda x) \sin(\mu y), \end{aligned} \tag{29a}$$

$$\begin{aligned} \sigma_{yy}^{(k)} = & -\left\{c_{12}^{(k)}\lambda U_{ij} + c_{22}^{(k)}\mu V_{ij} - z\left(c_{12}^{(k)}\lambda^2 + c_{22}^{(k)}\mu^2\right)W_{ij}\right. \\ & + \Psi(z)\cdot\left(c_{12}^{(k)}\lambda X_{ij} + c_{22}^{(k)}\mu Y_{ij}\right) + \left(c_{12}^{(k)}\alpha_x + c_{22}^{(k)}\alpha_y\right) \\ & \times [\bar{T}_1 + \bar{z}\bar{T}_2 - T_0] + \left(c_{12}^{(k)}\beta_x + c_{22}^{(k)}\beta_y\right) \\ & \times [\bar{C}_1 + \bar{z}\bar{C}_2 - C_0]\} \sin(\lambda x) \sin(\mu y), \end{aligned} \tag{29b}$$

$$\tau_{xy}^{(k)} = c_{66}^{(k)} \{ \mu U_{ij} + \lambda V_{ij} - 2z\lambda\mu W_{ij} \} \cos(\lambda x) \cos(\mu y). \tag{29c}$$

5 Numerical results and discussions

To verify the analytical formulation presented in the previous section, a variety of sample problems is considered. For the sake of brevity, only linearly varying (across the thickness) temperature distribution $T = T_1 + \bar{z}T_2$ and moisture distribution $C = C_1 + \bar{z}C_2$, non-linearly varying (across the thickness) temperature distribution $T = \bar{\Psi}(z)T_3$ and moisture distribution $C = \bar{\Psi}(z)C_3$. Finally a combination of both $T = T_1 + \bar{z}T_2 + \bar{\Psi}(z)T_3$ and $C = C_1 + \bar{z}C_2 + \bar{\Psi}(z)C_3$ are considered. In what follows, the reference temperature T_0 and moisture concentration C_0 are dropped. The improvement in the prediction of displacements and stresses by the present unified theory will be discussed. In all our problems, the lamina properties are assumed to be (Jacquemin and Vautrin 2002):

$$\begin{aligned} E_x &= 181 \text{ GPa}, \quad E_y = E_z = 10.3 \text{ GPa}, \\ G_{xy} = G_{xz} &= 7.17 \text{ GPa}, \quad G_{yz} = 2.39 \text{ GPa}, \\ \nu_{xy} = \nu_{xz} &= 0.28, \quad \nu_{yz} = 0.43, \\ \alpha_x &= 0.02 \times 10^{-6} / ^\circ\text{C}, \quad \alpha_y = \alpha_z = 22.5 \times 10^{-6} / ^\circ\text{C}, \\ \beta_x &= 0, \quad \beta_y = \beta_z = 0.6 \text{ (wt.\% H}_2\text{O)}^{-1}. \end{aligned}$$

Computations are carried out for the fundamental mode (i.e., $i = j = 1$). All of the lamina are assumed to be of the same thickness and made of the same orthotropic material. We will assume in all of the analyzed cases (unless otherwise stated) that $q = 0, a/h = 5, a/b = 2, \bar{T}_1 = 0, \bar{T}_2 = 300$, and $\bar{C}_1 = \bar{C}_3 = 0$. The thermal parameter $\tau = \bar{T}_3/\bar{T}_2$ may be takes a constant value. The dimensionless deflections due to hygrothermal conditions are given by

$$\bar{u}_3 = \frac{h^2}{\alpha_1 \bar{T}_2 a^3} u_3, \quad \hat{u}_3 = \frac{h}{100 \alpha_1 \bar{T}_2 a^2} u_3.$$

In addition, the following dimensionless stresses have been used throughout the tables and figures:

$$\begin{aligned} \bar{\sigma}_1 &= -\frac{1}{100\alpha_1 \bar{T}_2 E_1} \sigma_x \left(\frac{a}{2}, \frac{b}{2}, \frac{z}{h} \right), \\ \bar{\sigma}_2 &= -\frac{1}{10\alpha_1 \bar{T}_2 E_1} \sigma_y \left(\frac{a}{2}, \frac{b}{2}, \frac{z}{h} \right), \\ \bar{\sigma}_3 &= \frac{h}{\alpha_1 \bar{T}_2 E_1 a} \sigma_z \left(\frac{a}{2}, \frac{b}{2}, \frac{z}{h} \right), \\ \bar{\sigma}_4 &= -\frac{1}{\alpha_1 \bar{T}_2 E_1} \tau_{yz} \left(\frac{a}{2}, 0, \frac{z}{h} \right), \\ \bar{\sigma}_5 &= \frac{1}{10\alpha_1 \bar{T}_2 E_1} \tau_{xz} \left(0, \frac{b}{2}, \frac{z}{h} \right), \\ \bar{\sigma}_6 &= -\frac{1}{100\alpha_1 \bar{T}_2 E_1} \tau_{xy} \left(0, 0, \frac{z}{h} \right). \end{aligned}$$

Table 1 shows the effect of thickness on the dimensionless center deflections \hat{u}_3 of two-layer ($0^\circ/90^\circ$) cross-ply square plates subjected to sinusoidal hygrothermal or thermal conditions. The hygrothermal environment, affects on the center deflections \hat{u}_3 more than the thermal one. It is to be noted that, the hygrothermal deflections may be twice the thermal ones. Table 2 shows a comparison of the dimensionless center deflections \hat{u}_3 of four-layer anti-symmetric cross-ply ($0^\circ/90^\circ/0^\circ/90^\circ$) rectangular plates subjected to sinusoidal hygrothermal distribution linearly varying through the plate thickness. In addition, Table 2 contains the center deflections \hat{u}_3 that are caused by a sinusoidal temperature distribution linearly varying through the thickness. The hygrothermal environment affects more on the deflections than the thermal one. Generally, the difference between hygrothermal and thermal results for all theories are decreasing as the aspect ratio increases. The deflection due to CPT for both hygrothermal and thermal cases has the same value for all values of the ratio a/h . The deflection of the square plate shows the highest sensitivity. It is clear that for both hygrothermal and thermal results, the RPT yields the smallest deflections. The HPT and SPT yield very close results to each other.

Table 3 shows the effect of thickness on the dimensionless stresses of two-layer cross-ply rectangular plates subjected to combine sinusoidal hygrothermal conditions. The FPT gives the smallest normal stress $\bar{\sigma}_1$ and the transverse in-plane stress $\bar{\sigma}_6$ while it gives highest longitudinal stress $\bar{\sigma}_2$. As it is already known, the FPT gives the smallest and uniform shear stresses $\bar{\sigma}_5$ and $\bar{\sigma}_5$. The CPT gives reliable results only

Table 1 Effect of thickness on the dimensionless center deflection \hat{u}_3 of cross-ply (0°/90°) square plates in hygrothermal environment ($\tau = 0$)

| a/h | $\bar{C}_2 = 0 (0.507968)^a$ | | | | $\bar{C}_2 = 0.01(0.959164)^a$ | | | |
|-------|------------------------------|----------|----------|----------|--------------------------------|----------|----------|----------|
| | FPT | HPT | SPT | RPT | FPT | HPT | SPT | RPT |
| 100 | 0.507968 | 0.507971 | 0.507971 | 0.421048 | 0.959164 | 0.959169 | 0.959170 | 0.794982 |
| 50 | 0.507968 | 0.507978 | 0.507980 | 0.420947 | 0.959164 | 0.959184 | 0.959186 | 0.794790 |
| 25 | 0.507968 | 0.508009 | 0.508014 | 0.420540 | 0.959164 | 0.959241 | 0.959250 | 0.794022 |
| 20 | 0.507968 | 0.508031 | 0.508039 | 0.420234 | 0.959164 | 0.959284 | 0.959297 | 0.793443 |
| 15 | 0.507968 | 0.508081 | 0.508095 | 0.419570 | 0.959164 | 0.959377 | 0.959403 | 0.792190 |
| 10 | 0.507968 | 0.508221 | 0.508252 | 0.417658 | 0.959164 | 0.959641 | 0.959700 | 0.788578 |
| 5 | 0.507968 | 0.508972 | 0.509094 | 0.406911 | 0.959164 | 0.961059 | 0.961289 | 0.768277 |

^a Numbers between parentheses are given based on the CPT

Table 2 The dimensionless center deflections \hat{u}_3 of (0°/90°/0°/90°) rectangular plates in hygrothermal or thermal environment ($\tau = 0, \bar{C}_2 = 0.01$)

| a/h | Theory | $a/b = 1/3$ | $a/b = 0.5$ | $a/b = 1$ | $a/b = 1.5$ | $a/b = 2$ |
|-------|--------|-------------------|-------------------|-------------------|-------------------|-------------------|
| 5 | FPT | 0.49694 (0.26353) | 0.76870 (0.40736) | 1.00357 (0.53145) | 0.70098 (0.37120) | 0.46019 (0.24368) |
| | HPT | 0.50098 (0.26567) | 0.77290 (0.40958) | 1.00271 (0.53105) | 0.70047 (0.37093) | 0.46079 (0.24399) |
| | SPT | 0.50144 (0.26591) | 0.77332 (0.40980) | 1.00259 (0.53099) | 0.70048 (0.37093) | 0.46095 (0.24408) |
| | RPT | 0.35943 (0.19073) | 0.63077 (0.33434) | 0.89567 (0.47438) | 0.62846 (0.33280) | 0.40644 (0.21522) |
| 10 | FPT | 0.42533 (0.22562) | 0.66959 (0.35490) | 1.00347 (0.53145) | 0.73054 (0.38684) | 0.47932 (0.25379) |
| | HPT | 0.42670 (0.22635) | 0.67137 (0.35584) | 1.00328 (0.53135) | 0.72986 (0.38647) | 0.47904 (0.25364) |
| | SPT | 0.42688 (0.22644) | 0.67158 (0.35595) | 1.00325 (0.53134) | 0.72978 (0.38643) | 0.47901 (0.25363) |
| | RPT | 0.31082 (0.16500) | 0.55354 (0.29346) | 0.91576 (0.48502) | 0.67827 (0.35916) | 0.44622 (0.23627) |
| 20 | FPT | 0.40498 (0.21485) | 0.63898 (0.33869) | 1.00347 (0.53145) | 0.74378 (0.39384) | 0.48841 (0.25860) |
| | HPT | 0.40535 (0.21505) | 0.63948 (0.33896) | 1.00343 (0.53143) | 0.74353 (0.39371) | 0.48828 (0.25853) |
| | SPT | 0.40540 (0.21507) | 0.63954 (0.33899) | 1.00342 (0.53142) | 0.74350 (0.39369) | 0.48826 (0.25852) |
| | RPT | 0.29580 (0.15705) | 0.52769 (0.27978) | 0.92062 (0.48759) | 0.69699 (0.36907) | 0.46063 (0.24389) |
| 50 | FPT | 0.39908 (0.21173) | 0.62988 (0.33388) | 1.00347 (0.53145) | 0.74827 (0.39622) | 0.49158 (0.26027) |
| | HPT | 0.39914 (0.21176) | 0.62996 (0.33392) | 1.00347 (0.53145) | 0.74823 (0.39619) | 0.49155 (0.26026) |
| | SPT | 0.39915 (0.21177) | 0.62997 (0.33393) | 1.00346 (0.53145) | 0.74822 (0.39619) | 0.49155 (0.26026) |
| | RPT | 0.29135 (0.15470) | 0.51987 (0.27564) | 0.92196 (0.48830) | 0.70311 (0.37231) | 0.46534 (0.24639) |
| 100 | FPT | 0.39823 (0.21128) | 0.62856 (0.33318) | 1.00347 (0.53145) | 0.74895 (0.39658) | 0.49205 (0.26053) |
| | HPT | 0.39825 (0.21129) | 0.62858 (0.33319) | 1.00347 (0.53145) | 0.74894 (0.39657) | 0.49205 (0.26052) |
| | SPT | 0.39825 (0.21129) | 0.62858 (0.33319) | 1.00347 (0.53145) | 0.74894 (0.39657) | 0.49205 (0.26052) |
| | RPT | 0.29071 (0.15436) | 0.51873 (0.27503) | 0.92215 (0.48840) | 0.70403 (0.37279) | 0.46606 (0.24677) |
| | CPT | 0.39795 (0.21113) | 0.62812 (0.33295) | 1.00347 (0.53145) | 0.74918 (0.39670) | 0.49222 (0.26061) |

The numbers between parentheses are given for the thermal deflections ($\bar{C}_2 = 0$)

for thin plates. The other shear deformation theories HPT and SPT give stresses very close to each other with small relative error than the RPT. However, the RPT gives the accurate stresses.

Figure 2 shows the variation of dimensionless deflection \bar{u}_3 with side-to-thickness ratio for a four-

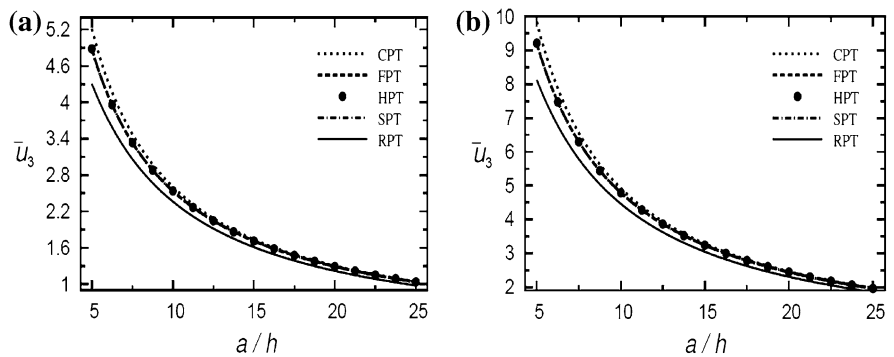
layer anti-symmetric (0°/90°/0°/90°) cross-ply rectangular plate in thermal or hygrothermal environment. The existence of moisture in the hygrothermal case affects more on the center deflections than thermal one. For both cases, the deflection decreases rapidly with the increasing of the ratio a/h . The FPT, HPT and

Table 3 The dimensionless stresses of (0°/90°) rectangular plates in hygrothermal or thermal environment ($\tau = 0, \bar{C}_2 = 0.01$)

| a/h | Theory | $\bar{\sigma}_1(-0.5)$ | $\bar{\sigma}_2(0.25)$ | $\bar{\sigma}_6(-0.5)$ | $\bar{\sigma}_4(0)$ | $\bar{\sigma}_5(0)$ |
|-------|--------|------------------------|------------------------|------------------------|---------------------|---------------------|
| 5 | FPT | 0.60741 (0.32049) | 1.77140 (0.93732) | 2.65162 (1.40485) | 2.24970 (1.18992) | 1.34982 (0.71395) |
| | HPT | 0.80752 (0.42632) | 1.17467 (0.62169) | 2.78924 (1.47764) | 2.77808 (1.46937) | 1.67991 (0.88856) |
| | SPT | 0.82310 (0.43457) | 1.11033 (0.58766) | 2.80083 (1.48377) | 2.85837 (1.51184) | 1.73277 (0.91652) |
| | RPT | 0.85345 (0.45063) | 1.30117 (0.68872) | 2.47666 (1.31214) | 2.91788 (1.54331) | 1.87776 (0.99326) |
| 10 | FPT | 1.10195 (0.58206) | 2.20182 (1.16498) | 2.92694 (1.55047) | 1.62141 (0.85760) | 0.97285 (0.51456) |
| | HPT | 1.17634 (0.62139) | 1.99217 (1.05408) | 2.97770 (1.57732) | 1.97647 (1.04539) | 1.19837 (0.63385) |
| | SPT | 1.18212 (0.62446) | 1.96976 (1.04223) | 2.98195 (1.57957) | 2.03210 (1.07482) | 1.23431 (0.65287) |
| | RPT | 1.18026 (0.62346) | 1.38594 (0.73311) | 2.62332 (1.38968) | 2.06303 (1.09116) | 1.35297 (0.71567) |
| 20 | FPT | 1.30227 (0.68801) | 2.37617 (1.25719) | 3.03846 (1.60946) | 0.91128 (0.48199) | 0.54677 (0.28920) |
| | HPT | 1.32342 (0.69920) | 2.31784 (1.22634) | 3.05285 (1.61707) | 1.10540 (0.58467) | 0.67068 (0.35475) |
| | SPT | 1.32507 (0.70007) | 2.31163 (1.22306) | 3.05406 (1.61771) | 1.13609 (0.60090) | 0.69042 (0.3651) |
| | RPT | 1.32124 (0.69803) | 1.55089 (0.82024) | 2.69220 (1.42610) | 1.15795 (0.61245) | 0.75907 (0.40152) |
| 50 | FPT | 1.36759 (0.72256) | 2.43302 (1.28726) | 3.07482 (1.62869) | 0.37763 (0.19974) | 0.22658 (0.11984) |
| | HPT | 1.37111 (0.72442) | 2.42338 (1.28216) | 3.07721 (1.62995) | 0.45735 (0.24190) | 0.27755 (0.14680) |
| | SPT | 1.37138 (0.72457) | 2.42236 (1.28162) | 3.07741 (1.63006) | 0.46999 (0.24859) | 0.28566 (0.15110) |
| | RPT | 1.36782 (0.72267) | 1.61453 (0.85387) | 2.71534 (1.43834) | 0.47978 (0.25376) | 0.31435 (0.16628) |
| 100 | FPT | 1.37730 (0.72770) | 2.44147 (1.29173) | 3.08023 (1.63155) | 0.18979 (0.10038) | 0.11387 (0.06023) |
| | HPT | 1.37819 (0.72817) | 2.43905 (1.29045) | 3.08083 (1.63187) | 0.22981 (0.12155) | 0.13946 (0.07377) |
| | SPT | 1.37826 (0.72820) | 2.43880 (1.29032) | 3.08088 (1.63189) | 0.23615 (0.12491) | 0.14354 (0.07592) |
| | RPT | 1.37477 (0.72634) | 1.62435 (0.85906) | 2.71881 (1.44018) | 0.24113 (0.12753) | 0.15797 (0.08356) |
| | CPT | 1.38057 (0.72942) | 2.44431 (1.29324) | 3.08204 (1.63251) | – | – |

The numbers between parentheses are given for the thermal stresses ($\bar{C}_2 = 0$)

Fig. 2 Effect of thickness on the dimensionless deflection \bar{u}_3 of a four-layer, anti-symmetric cross-ply (0°/90°/0°/90°) rectangular plate: **a** $\bar{C}_2 = 0$, **b** $\bar{C}_2 = 0.01$



SPT yield closer results while RPT gives the accurate deflections and the CPT gives appropriate deflections especially after greater values of a/h .

The deflection due to the RPT is plotting through-the-thickness of the (0°/90°/0°/90°) rectangular plate in Fig. 3 according some values of the thermal parameter τ . The deflection is very sensitive to its position through the plate thickness. This does not occur for deflections due to other theories which they are independent of the z -axis. In addition, the

deflection increases with the increase of the thermal parameter value. The present RPT also gives the transverse normal stress $\bar{\sigma}_3$ alone. Figures 4 and 5 plot this stress through-the-thickness of (0°/90°) and (0°/90°/0°/90°) rectangular plates, respectively. These figures allow themselves to underline their great influence on transverse normal stress through-the-thickness of different plates. The sensitivity of the thermal parameter on $\bar{\sigma}_3$ is also showed in these figures.

Fig. 3 The deflection \bar{u}_3 due to RPT through-the-thickness of a $(0^\circ/90^\circ/0^\circ/90^\circ)$ rectangular plate for various values of τ : **a** $\bar{C}_2 = 0$, **b** $\bar{C}_2 = 0.01$

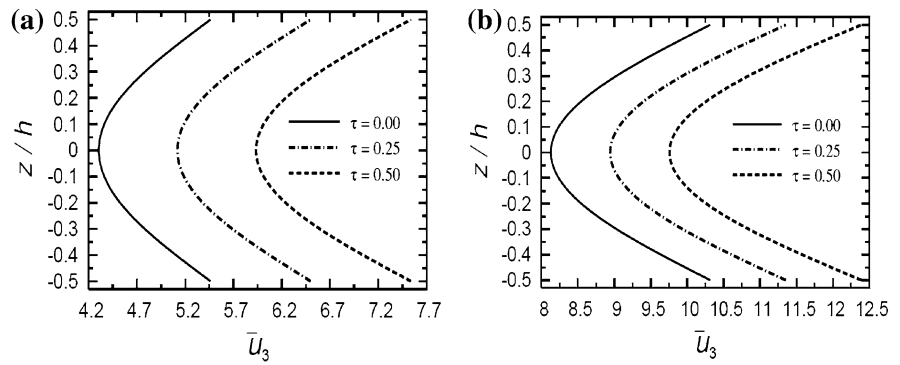


Fig. 4 The distribution of dimensionless normal stress $\bar{\sigma}_3$ through the thickness of a $(0^\circ/90^\circ)$ rectangular plate for various values of τ : **a** $\bar{C}_2 = 0$, **b** $\bar{C}_2 = 0.01$

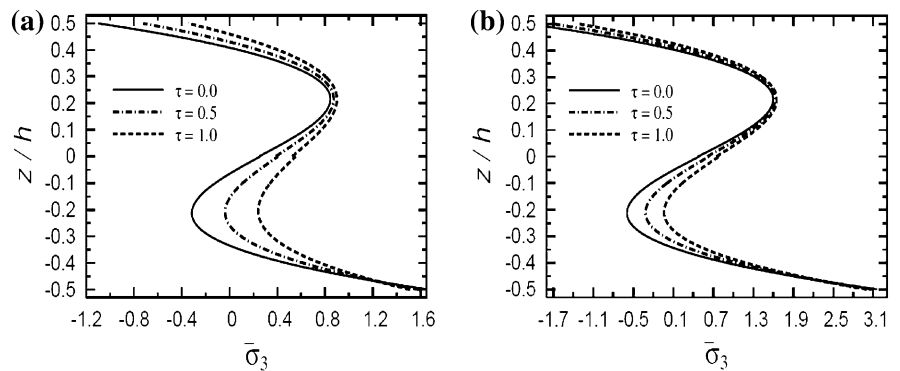


Fig. 5 The distribution of dimensionless normal stress $\bar{\sigma}_3$ through the thickness of a $(0^\circ/90^\circ/0^\circ/90^\circ)$ rectangular plate for various values of τ : **a** $\bar{C}_2 = 0$, **b** $\bar{C}_2 = 0.01$.

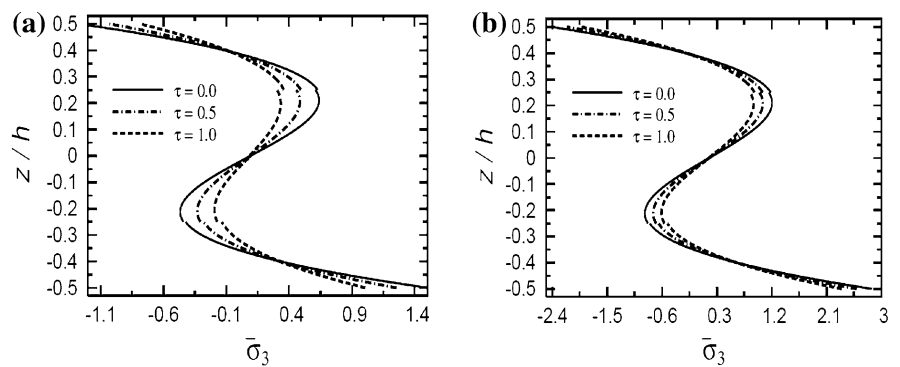


Fig. 6 The distribution of dimensionless shear stress $\bar{\sigma}_4$ through the thickness of a $(0^\circ/90^\circ/0^\circ/90^\circ)$ rectangular plate: **a** $\bar{C}_2 = 0$, **b** $\bar{C}_2 = 0.01$

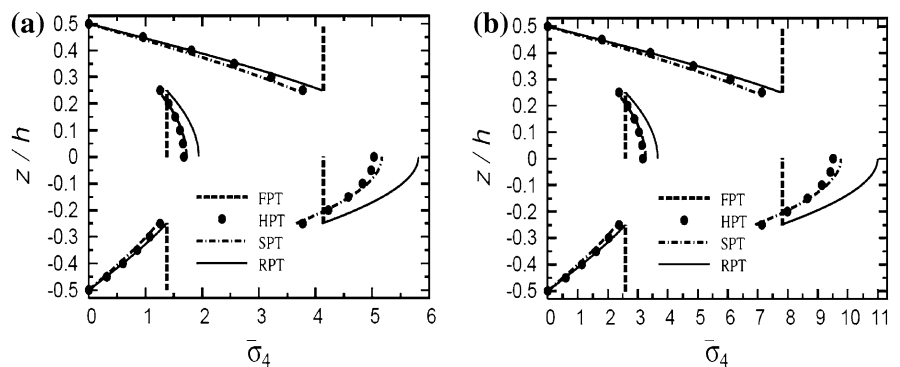


Fig. 7 The distribution of dimensionless shear stress $\bar{\sigma}_5$ through the thickness of a $(0^\circ/90^\circ/0^\circ/90^\circ)$ rectangular plate: **a** $\bar{C}_2 = 0$, **b** $\bar{C}_2 = 0.01$

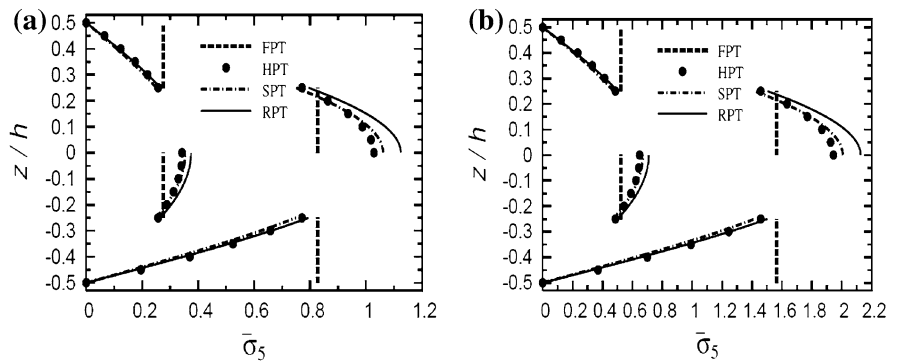


Figure 6 shows the distribution of transverse shear stress $\bar{\sigma}_4$ through the thickness of a four-layer cross-ply anti-symmetric $(0^\circ/90^\circ/0^\circ/90^\circ)$ rectangular plate due to both thermal and hygrothermal effects. The distribution of transverse shear stress $\bar{\sigma}_5$ through the thickness of $(0^\circ/90^\circ/0^\circ/90^\circ)$ cross-ply anti-symmetric rectangular plate due to both thermal and hygrothermal effects is also shown in Fig. 7. The results displayed in these figures show that the stress continuity across each layer interface is not imposed in the present theories. The FPT may be insufficient for transverse shear stresses while HPT and SPT gives very close results to each other. The disagreement between HPT and RPT, especially at the plate center, is owing to the higher-order contributions of RPT.

6 Conclusions

The static response of antisymmetric cross-ply laminated plates is discussed analytically and numerical results are given using a unified theory. The present plate is subjected to sinusoidally non-uniform distributions of temperature and moisture concentrations. Analytical solutions for governing differential equations of simply-supported laminates are developed using Navier’s procedure and separation of variable technique. The dimensionless deflections and stresses are computed and compared using various plate theories. It was found that, the CPT predicts deflections and stresses, as it is expected, significantly different from those of the shear deformation theories. The FPT results are less accurate in prediction of deflections and stresses than other shear deformation theories. In some cases, the HPT gives transverse shear stresses with relative errors comparing with SPT and RPT. In most problems the HPT and SPT give

close results to each other. However, RPT gives more accurate results and that is due to the influences of transverse normal strain in this theory.

Appendix 1

The elements of the symmetric matrix $[L]$, for RPT, are given by:

$$\begin{aligned}
 L_{11} &= A_{11}d_{11} + 2A_{16}d_{12} + A_{66}d_{22}, \\
 L_{12} &= A_{16}d_{11} + (A_{12} + A_{66})d_{12} + A_{26}d_{22}, \\
 L_{13} &= -B_{11}d_{111} - 3B_{16}d_{112} - (B_{12} + 2B_{66})d_{122} - B_{26}d_{222}, \\
 L_{14} &= B_{11}^a d_{11} + 2B_{16}^a d_{12} + B_{66}^a d_{22}, \\
 L_{15} &= B_{16}^a d_{11} + (B_{12}^a + B_{66}^a)d_{12} + B_{26}^a d_{22}, \\
 L_{16} &= L_{13}^a d_1 + L_{63}^a d_2, \\
 L_{22} &= A_{66}d_{11} + 2A_{26}d_{12} + A_{22}d_{22}, \\
 L_{23} &= -B_{16}d_{111} - (B_{12} + 2B_{66})d_{112} - 3B_{26}d_{122} - B_{22}d_{222}, \\
 L_{24} &= L_{15}, \\
 L_{25} &= B_{66}^a d_{11} + 2B_{26}^a d_{12} + B_{22}^a d_{22}, \\
 L_{26} &= L_{63}^a d_1 + L_{23}^a d_2, \\
 L_{33} &= D_{11}d_{1111} + 4D_{16}d_{1112} + 2(D_{12} + 2D_{66})d_{1122} \\
 &\quad + 4D_{26}d_{1222} + D_{22}d_{2222}, \\
 L_{34} &= -D_{11}^a d_{111} - 3D_{16}^a d_{112} - (D_{12}^a + 2D_{66}^a)d_{122} - D_{26}^a d_{222}, \\
 L_{35} &= -D_{16}^a d_{111} - (D_{12}^a + 2D_{66}^a)d_{112} - 3D_{26}^a d_{122} - D_{22}^a d_{222}, \\
 L_{36} &= -(\bar{L}_{13}d_{11} + 2\bar{L}_{63}d_{12} + \bar{L}_{23}d_{22}), \\
 L_{44} &= F_{11}^a d_{11} + 2F_{16}^a d_{12} + F_{66}^a d_{22} - A_{55}^a, \\
 L_{45} &= F_{16}^a d_{11} + (F_{12}^a + F_{66}^a)d_{12} + F_{26}^a d_{22} - A_{45}^a, \\
 L_{46} &= (\hat{L}_{13} - A_{55}^a)d_1 + (\hat{L}_{63} - A_{45}^a)d_2, \\
 L_{55} &= F_{66}^a d_{11} + 2F_{26}^a d_{12} + F_{22}^a d_{22} - A_{44}^a, \\
 L_{56} &= (\hat{L}_{63} - A_{45}^a)d_1 + (\hat{L}_{23} - A_{44}^a)d_2, \\
 L_{66} &= -(A_{55}^a d_1 + 2A_{45}^a d_{12} + A_{44}^a d_{22} - \tilde{L}_{33}).
 \end{aligned}$$

For the FPT, HPT and SPT, the components of $[L]$ are the same as given above for the RPT except $L_{i6} = 0 (i = 1, 2, \dots, 6)$. However, for the CPT, the

components of $[L]$ are reduced to be $L_{ij}(i, j = 1, 2, 3)$.

Appendix 2

The transformation formulae for the stiffness $c_{ij}^{(k)}$ are

$$\begin{Bmatrix} c_{11} \\ c_{12} \\ c_{22} \\ c_{16} \\ c_{26} \\ c_{66} \end{Bmatrix}^{(k)} = \begin{bmatrix} c^4 & 2c^2s^2 & s^4 & 4c^2s^2 \\ c^2s^2 & c^4 + s^4 & c^2s^2 & -4c^2s^2 \\ s^4 & 2c^2s^2 & c^4 & 4c^2s^2 \\ c^3s & cs^3 - c^3s & -cs^3 & -2cs(c^2 - s^2) \\ cs^3 & c^3s - cs^3 & -c^3s & 2cs(c^2 - s^2) \\ c^2s^2 & -2c^2s^2 & c^2s^2 & (c^2 - s^2)^2 \end{bmatrix} \begin{Bmatrix} c_{11} \\ c_{12} \\ c_{22} \\ c_{66} \end{Bmatrix},$$

$$\begin{Bmatrix} c_{44} \\ c_{45} \\ c_{55} \end{Bmatrix}^{(k)} = \begin{bmatrix} c^2 & s^2 \\ -cs & cs \\ s^2 & c^2 \end{bmatrix} \begin{Bmatrix} c_{44} \\ c_{55} \end{Bmatrix}, \quad \begin{Bmatrix} c_{13} \\ c_{23} \\ c_{63} \end{Bmatrix}^{(k)} = \begin{bmatrix} c^2 & s^2 \\ s^2 & c^2 \\ sc & -sc \end{bmatrix} \begin{Bmatrix} c_{13} \\ c_{23} \end{Bmatrix}, \quad c_{33}^{(k)} = c_{33},$$

where $c = \cos \theta_k$, $s = \sin \theta_k$ and c_{ij} are the material stiffness of the lamina. For RPT one has

$$\begin{aligned} c_{11} &= \frac{E_x(1 - \nu_{yz}\nu_{zy})}{\Delta}, & c_{12} &= \frac{E_x(\nu_{yx} + \nu_{yz}\nu_{zx})}{\Delta}, \\ c_{13} &= \frac{E_x(\nu_{zx} + \nu_{yx}\nu_{zy})}{\Delta}, & c_{22} &= \frac{E_y(1 - \nu_{xz}\nu_{zx})}{\Delta}, \\ c_{23} &= \frac{E_y(\nu_{zy} + \nu_{xy}\nu_{zx})}{\Delta}, & c_{33} &= \frac{E_z(1 - \nu_{xy}\nu_{yx})}{\Delta}, \\ c_{44} &= G_{yz}, & c_{55} &= G_{xz}, & c_{66} &= G_{xy}. \end{aligned}$$

in which $\Delta = 1 - \nu_{xy}\nu_{yx} - \nu_{yz}\nu_{zy} - \nu_{zx}\nu_{xz} - 2\nu_{yx}\nu_{xz}\nu_{zy}$, E_i are Young's moduli in the material principal directions, ν_{ij} are Poisson's ratios and G_{ij} are shear moduli. The material stiffness for the CPT and other shear deformation plate theories may be reduced to:

$$\begin{aligned} c_{11} &= \frac{E_x}{1 - \nu_{xy}\nu_{yx}}, & c_{12} &= \frac{\nu_{xy}E_y}{1 - \nu_{xy}\nu_{yx}} = \frac{\nu_{yx}E_x}{1 - \nu_{xy}\nu_{yx}}, \\ c_{22} &= \frac{E_y}{1 - \nu_{xy}\nu_{yx}}, & c_{13} &= \frac{\nu_{xz}E_z}{1 - \nu_{xy}\nu_{yx}}, & c_{23} &= \frac{\nu_{yz}E_z}{1 - \nu_{xy}\nu_{yx}}, \\ c_{33} &= \frac{E_z}{1 - \nu_{xy}\nu_{yx}}, & c_{44} &= G_{yz}, & c_{55} &= G_{xz}, & c_{66} &= G_{xy}. \end{aligned}$$

Appendix 3

The components of the generalized force vector $\{F\}$ are given by

$$\begin{aligned} F_1^{ij} &= \lambda(A_1^T \bar{T}_1 + B_1^T \bar{T}_2 + {}^a B_1^T \bar{T}_3 + a_1^T \bar{C}_1 \\ &\quad + b_1^T \bar{C}_2 + {}^a b_1^T \bar{C}_3), \\ F_2^{ij} &= \mu(A_2^T \bar{T}_1 + B_2^T \bar{T}_2 + {}^a B_2^T \bar{T}_3 + a_2^T \bar{C}_1 \\ &\quad + b_2^T \bar{C}_2 + {}^a b_2^T \bar{C}_3), \\ F_3^{ij} &= -q_0 - h[(B_1^T \lambda^2 + B_2^T \mu^2) \bar{T}_1 \\ &\quad + (D_1^T \lambda^2 + D_2^T \mu^2) \bar{T}_2 \\ &\quad + ({}^a D_1^T \lambda^2 + {}^a D_2^T \mu^2) \bar{T}_3 + (b_1^T \lambda^2 + b_2^T \mu^2) \bar{C}_1 \\ &\quad + (d_1^T \lambda^2 + d_2^T \mu^2) \bar{C}_2 + ({}^a d_1^T \lambda^2 + {}^a d_2^T \mu^2) \bar{C}_3], \\ F_4^{ij} &= h\lambda({}^a B_1^T \bar{T}_1 + {}^a D_1^T \bar{T}_2 + {}^a F_1^T \bar{T}_3 + {}^a b_1^T \bar{C}_1 \\ &\quad + {}^a d_1^T \bar{C}_2 + {}^a f_1^T \bar{C}_3), \\ F_5^{ij} &= h\mu({}^a B_2^T \bar{T}_1 + {}^a D_2^T \bar{T}_2 + {}^a F_2^T \bar{T}_3 + {}^a B_2^T \bar{C}_1 \\ &\quad + {}^a D_2^T \bar{C}_2 + {}^a F_2^T \bar{C}_3), \\ F_6^{ij} &= -h(L^T \bar{T}_1 + {}^a L^T \bar{T}_2 + {}^b L^T \bar{T}_3 + l^T \bar{C}_1 \\ &\quad + {}^a l^T \bar{C}_2 + {}^b l^T \bar{C}_3), \end{aligned}$$

where

$$\{A_i^T, B_i^T, D_i^T\} = \sum_{k=1}^n \int_{z_k}^{z_{k+1}} (c_{1i}^{(k)} \alpha_x + c_{i2}^{(k)} \alpha_y) \{1, \bar{z}, \bar{z}^2\} dz, \quad (i = 1, 2),$$

$$\{a_i^T, b_i^T, d_i^T\} = \sum_{k=1}^n \int_{z_k}^{z_{k+1}} (c_{1i}^{(k)} \beta_x + c_{i2}^{(k)} \beta_y) \{1, \bar{z}, \bar{z}^2\} dz, \quad (i = 1, 2),$$

$$\{^a B_i^T, ^a D_i^T, ^a F_i^T\} = \sum_{k=1}^n \int_{z_k}^{z_{k+1}} (c_{1i}^{(k)} \alpha_x + c_{i2}^{(k)} \alpha_y) \bar{\Psi}(z) \{1, \bar{z}, \bar{\Psi}(z)\} dz, \quad (i = 1, 2),$$

$$\{^a b_i^T, ^a d_i^T, ^a f_i^T\} = \sum_{k=1}^n \int_{z_k}^{z_{k+1}} (c_{1i}^{(k)} \beta_x + c_{i2}^{(k)} \beta_y) \bar{\Psi}(z) \{1, \bar{z}, \bar{\Psi}(z)\} dz, \quad (i = 1, 2),$$

$$\{L^T, ^a L^T, ^b L^T\} = \sum_{k=1}^n \int_{z_k}^{z_{k+1}} (c_{13}^{(k)} \alpha_x + c_{23}^{(k)} \alpha_y) \bar{\Psi}''(z) \{1, \bar{z}, \bar{\Psi}(z)\} dz,$$

$$\{l^T, ^a l^T, ^b l^T\} = \sum_{k=1}^n \int_{z_k}^{z_{k+1}} (c_{13}^{(k)} \beta_x + c_{23}^{(k)} \beta_y) \bar{\Psi}''(z) \{1, \bar{z}, \bar{\Psi}(z)\} dz,$$

in which $\bar{z} = z/h$, $\bar{\Psi}(z) = \Psi(z)/h$, and $\bar{\Psi}''(z) = \Psi''(z)/h$.

The elements of the symmetric matrix $[C]$, for RPT, are given by:

$$C_{11} = -A_{11} \lambda^2 - A_{66} \mu^2,$$

$$C_{12} = -(A_{12} + A_{66}) \lambda \mu,$$

$$C_{13} = \lambda [B_{11} \lambda^2 + (B_{12} + 2B_{66}) \mu^2],$$

$$C_{14} = -B_{11}^a \lambda^2 - B_{66}^a \mu^2,$$

$$C_{15} = -(B_{12}^a + B_{66}^a) \lambda \mu,$$

$$C_{16} = L_{13}^a \lambda,$$

$$C_{22} = -A_{66} \lambda^2 - A_{22} \mu^2,$$

$$C_{23} = \mu [(B_{12} + 2B_{66}) \lambda^2 + B_{22} \mu^2],$$

$$C_{24} = C_{15},$$

$$C_{25} = -B_{66}^a \lambda^2 - B_{22}^a \mu^2,$$

$$C_{26} = L_{23}^a \mu,$$

$$C_{33} = -D_{11} \lambda^4 - 2(D_{12} + 2D_{66}) \lambda^2 \mu^2 - D_{22} \mu^4,$$

$$C_{34} = \lambda [D_{11}^a \lambda^2 + (D_{12}^a + 2D_{66}^a) \mu^2],$$

$$C_{35} = \mu [(D_{12}^a + 2D_{66}^a) \lambda^2 + D_{22}^a \mu^2],$$

$$C_{36} = -(\bar{L}_{13} \lambda^2 + \bar{L}_{23} \mu^2),$$

$$C_{44} = -(F_{11}^a \lambda^2 + F_{66}^a \mu^2 + A_{55}^a),$$

$$C_{45} = -(F_{12}^a + F_{66}^a) \lambda \mu,$$

$$C_{46} = (\hat{L}_{13} - A_{55}^a) \lambda,$$

$$C_{55} = -F_{66}^a \lambda^2 - F_{22}^a \mu^2 - A_{44}^a,$$

$$C_{56} = (\hat{L}_{23} - A_{44}^a) \mu,$$

$$C_{66} = -(A_{55}^a \lambda^2 + A_{44}^a \mu^2 + \bar{L}_{33}).$$

For the FPT, HPT and SPT, the components of $[C]$ are the same as given above for the RPT except $C_{i6} = 0 (i = 1, 2, \dots, 6)$. However, for the CPT, the components of $[C]$ are reduced to be $C_{ij} (i, j = 1, 2, 3)$.

References

Ameur, M., Tounsi, A., Benyoucef, S., Bachir Bouiadjra, M., Adda Bedia, E.A.: Stress analysis of steel beams strengthened with a bonded hygrothermal aged composite plate. *Int. J. Mech. Mater. Des.* **5**, 143–156 (2009)

Atmane, H.A., Tounsi, A., Mechab, I., Adda Bedia, E.: Free vibration analysis of functionally graded plates resting on Winkler-Pasternak elastic foundations using a new shear deformation theory. *Int. J. Mech. Mater. Des.* **6**, 113–121 (2010)

Bahrami, A., Nosier, A.: Interlaminar hygrothermal stresses in laminated plates. *Int. J. Solids Struct.* **44**, 8119–8142 (2007)

Benkhedda, A., Tounsi, A., Adda Bedia, E.A.: Effect of temperature and humidity on transient hygrothermal stresses during moisture desorption in laminated composite plates. *Compos. Struct.* **82**, 623–635 (2008)

Carrera, E.: Historical review of zig-zag theories for multilayered plates and shells. *Appl. Mech. Rev.* **56**, 301–329 (2003)

Jacquemin, F., Vautrin, A.: A closed-form solution for the internal stresses in thick composite cylinders induced by cyclical environmental conditions. *Compos. Struct.* **58**, 1–9 (2002)

- Lee, S.Y., Chou, C.J., Jang, J.L., Lim, J.S.: Hygrothermal effects on the linear and nonlinear analysis of symmetric angle-ply laminated plates. *Compos. Struct.* **21**, 41–48 (1992)
- Pipes, R.B., Vinson, J.R., Chou, T.W.: On the hygrothermal response of laminated composite systems. *J. Compos. Mater.* **10**, 129–148 (1976)
- Rao, V.V.S., Sinha, P.K.: Bending characteristic of thick multidirectional composite plates under hygrothermal environment. *Reinf. Plast. Compos.* **23**, 1481–1495 (2004)
- Reddy, J.N.: A generalization of two-dimensional theories of laminated composite laminates. *Commun. Appl. Numer. Method* **3**, 173–180 (1987)
- Reddy, J.N.: A simple higher-order theory for laminated composite plates. *J. Appl. Mech.* **51**, 745–752 (1984)
- Sai Ram, K.S., Sinha, P.K.: Hygrothermal effects on the bending characteristics on laminated composite plates. *Comput. Struct.* **40**, 1009–1015 (1991)
- Sai Ram, K.S., Sinha, P.K.: Hygrothermal effects on the free vibration of laminated composite plates. *J. Sound Vib.* **158**, 133–148 (1992)
- Wang, X., Dong, K., Wang, X.Y.: Hygrothermal effect on dynamic interlaminar stresses in laminated plates with piezoelectric actuators. *Compos. Struct.* **71**, 220–228 (2005)
- Whitney, J.M., Ashton, J.E.: Effect of environment on the elastic response of layered composite plates. *AIAA J.* **9**, 1708–1713 (1971)
- Zenkour, A.M.: A comprehensive analysis of functionally graded sandwich plates: part 1: deflection and stresses. *Int. J. Solids Struct.* **42**, 5224–5242 (2005a)
- Zenkour, A.M., Alghamdi, N.A.: Thermoelastic bending analysis of functionally graded sandwich plates. *J. Mater. Sci.* **43**, 2574–2589 (2008)
- Zenkour, A.M., Allam, M.N.M., Radwan, A.F.: Bending of cross-ply laminated plates resting on elastic foundations under thermo-mechanical loading. *Int. J. Mech. Mater. Des.* **9**, 239–251 (2013)
- Zenkour, A.M.: Analytical solution for bending of cross-ply laminated plates under thermo-mechanical loading. *Compos. Struct.* **65**, 367–379 (2004a)
- Zenkour, A.M.: Benchmark trigonometric and 3-D elasticity solutions for an exponentially graded thick rectangular plate. *Arch. Appl. Mech.* **77**, 197–214 (2007)
- Zenkour, A.M.: Buckling of fiber-reinforced viscoelastic composite plates using various plate theories. *J. Eng. Math.* **50**, 75–93 (2004b)
- Zenkour, A.M.: Generalized shear deformation theory for bending analysis of functionally graded plates. *Appl. Math. Model.* **30**, 67–84 (2006)
- Zenkour, A.M.: On vibration of functionally graded plates according to a refined trigonometric plate theory. *Int. J. Struct. Stab. Dyn.* **5**, 279–297 (2005b)
- Zenkour, A.M.: Thermal effects on the bending response of fiber-reinforced viscoelastic composite plates using a sinusoidal shear deformation theory. *Acta Mech.* **171**, 171–187 (2004c)